Dyes and Pigments 167 (2019) 174–180

Contents lists available at ScienceDirect

Dyes and Pigments

journal homepage: www.elsevier.com/locate/dyepig

# Water-soluble polymeric probe with dual recognition sites for the sequential colorimetric detection of cyanide and Fe (III) ions

Moumita Gupta, Hyung-il Lee*

*Department of Chemistry, University of Ulsan, Ulsan, 680-749, Republic of Korea*

ARTICLE INFO

*Keywords:*
Dual sensor
Iron (III) sensor
Cyanide sensor
Polymeric probe
Colorimetric
Sequential detection

ABSTRACT

A water-soluble polymeric probe derived from an azo-Schiff base was developed for the consecutive colorimetric sensing of $CN^-$ and $Fe^{3+}$ ions in water. Herein, the synthesis of a random copolymer of *N,N*-dimethylacrylamide (DMA) and 3-vinylbenzaldehyde (VBA) via reversible addition-fragmentation chain transfer polymerization, [p(DMA-*co*-VBA, P1] is described. A post-polymerization modification reaction between the aldehyde groups of P1 and (E)-2-amino-4-((4-nitrophenyl)diazenyl)phenol in ethanol led to the target polymer, P2, with azo-Schiff base moieties. The colorimetric detection of $CN^-$ ions occurred because of the abstraction of phenolic proton of P2 by the $CN^-$ ions to form hydrazone, which was accompanied by the color change from brick-red to purple. The selective colorimetric detection of $Fe^{3+}$ ions with P2 over other cations in water was also observed via the formation of a coordination complex between $Fe^{3+}$ ions and azo-Schiff base ligands of P2. After the individual detection of $CN^-$ and $Fe^{3+}$ was carried out, consecutive sensing studies were performed. Although $Fe^{3+}$ was sequentially observed after the presence of $CN^-$ ions was noted, detection using a reverse sequence from $Fe^{3+}$ to $CN^-$ was not possible because of the intense color of the resulting P2−$Fe^{3+}$ complexes, which suppressed any observable color changes typically caused by the formation of hydrazone.

## 1. Introduction

Development of chemosensors for the efficient detection of $Fe^{3+}$ and toxic $CN^-$ ions has attracted considerable attention [1–4]. $Fe^{3+}$ ions not only provide the oxygen-carrying capacity of heme but also act as a cofactor in many enzymatic reactions in human body [5,6]. Deficiency or overdoses of this biologically important cation lead to Alzheimer's and Parkinson's diseases and various disorders in organs [7–9]. On the other hand, $CN^-$ ions released by many industrial and chemical processes are easily absorbed by the human body through the lungs, gastrointestinal tract, and skin, thereby causing many health problems [10–12]. The strong binding of $CN^-$ ions with iron in cytochrome *c* oxidase can result in premature death [13]. Thus, it is very important to develop molecular probes for the selective detection of $Fe^{3+}$ and $CN^-$ ions individually and sequentially.

The detection of these ions relies heavily on instrumental methods, including atomic absorption spectroscopy and inductively coupled plasma mass spectrometry [14]. Unfortunately, these techniques have numerous disadvantages, such as high costs, no portability, and lengthy times required for analysis. With this in mind, colorimetric and fluorometric chemosensors have been developed for the detection of various ions, thus widening the range of analytes that can be utilized [15–18]. Though various small molecular colorimetric probes have been developed for multi-ion sensing studies, they are not soluble in water [19,20]. Hence, evolution of the polymeric probes used for the quantitative and qualitative detection of multi-ions is very important for sensing the presence of toxic analytes in aqueous waste [21,22]. Moreover, polymers with sensor moieties in their polymeric backbones are more advanced systems than the small molecules typically used in such studies as they can be prepared and subsequently transferred into films and coatings, or designed into distinct geometries, such as linear, spherical, and crosslinked networks that enable the detection analytes both in liquid and vapor states [23].

Recently, a few polymeric probes have been developed for the colorimetric detection of $Fe^{3+}$ ions [24]. Visual color change due to the formation of co-ordination complexes between the sensing moiety and the analyte was observed. There are very few published reports for the detection of $Fe^{3+}$ ions, which are based on phosphonate-functionalized polyfluorene and acrylic polymers with different sensing units (such as kojic acids) [25,26]. On the other hand, numerous strategies have been implemented for the colorimetric detection of $CN^-$ ions, including H-bonding interactions [27], complex formations [28], nucleophilic attacks on activated C=O [29] and C=C [30], boron center [31], and deprotonation reactions [32,33].

* Corresponding author.
*E-mail address:* sims0904@ulsan.ac.kr (H.-i. Lee).

https://doi.org/10.1016/j.dyepig.2019.04.010
Received 28 February 2019; Received in revised form 5 April 2019; Accepted 5 April 2019
Available online 13 April 2019

Here, we report the synthesis of an azo-Schiff base-derived single polymeric probe, P2, that could be utilized for the colorimetric detection of both trivalent iron ($Fe^{3+}$) and $CN^-$ ions in aqueous media both individually and sequentially. The aldehyde functionalized polymer was post-modified with an amine-functionalized azo chromophore via imine bond chemistry. The imine bond and the adjacent phenolic–OH group are known to form coordination bonds with metals and undergo deprotonation and/or addition reactions with basic/nucleophilic anions. Thus, there is a degree of versatility in the application of said probes for the colorimetric detection of cations ($Fe^{3+}$ ions) and anions ($CN^-$ ions) by dual channel. Moreover, in sequential detection studies, the addition of $CN^-$ ions followed by $Fe^{3+}$ ions in this order allows for better detection of both ions, whereas addition in the reverse sequence leads to the $Fe^{3+}$ ions masking the subsequent detection of the $CN^-$ ions. Although different probes for individual detection of $CN^-$ and $Fe^{3+}$ ions have been documented previously, we report a novel polymeric chemosensor for the one-pot detection of $Fe^{3+}$ and $CN^-$ ions individually and sequentially.

## 2. Materials and methods

### 2.1. Materials

3-Vinylbenzaldehyde (VBA, 99.0%) and dimethyl acrylamide (DMA, 99.0%) were purchased from Aldrich and purified by passing through a column filled with basic alumina in order to remove any impurities. 2-Aminophenol, 4-nitroaniline, 2-dodecylsulfanylthiocarbonylsulfanyl-2-methylpropionic acid (DMP), *tert*-butyloxycarbonyl (BOC) anhydride, TFA (trifluoro acetic acid), all metal salts, HEPES (4-(2-hydroxyethyl)-1-piperazineethanesulfonic acid) buffer solution, and tetrabutyammonium salts were purchased from Aldrich at the highest purity available and were used as received. The solvents were obtained from commercial suppliers and were used as received. 2,2′-Azobis(isobutyronitrile) (AIBN, Aldrich, 98%) was recrystallized from ethanol.

### 2.2. Instrumentation

$^1$H-NMR spectra were collected in DMSO-$d_6$ using a Bruker Avance 300 MHz NMR spectrometer. The apparent molecular weight and molecular weight distributions were measured via gel permeation chromatography (GPC, Agilent Technologies 1200 series) using a polymethylmethachrylate standard with DMF (dimethyl formamide) as the eluent at 30 °C and at a flow rate of 1.00 mL/min. The UV–Vis absorption spectra were recorded using a Varian Cary-100 UV–Vis spectrophotometer.

### 2.3. Synthesis of tert-butyl (2-hydroxyphenyl)carbamate (S1)

To the solution of 2-aminophenol (1) (4 g, 36.6 mmol) in 60 mL THF–water (1:1 v/v) triethylamine ($Et_3N$) (9.8 mL, 44.1 mmol) was added. Then, BOC anhydride (8.4 mL, 36.6 mmol) was added and stirred overnight. The reaction mixture was diluted with water and subsequently extracted with ethyl acetate. The organic layer was dried over $Na_2SO_4$, and the solvent was evaporated. The crude mixture was purified via column chromatography (hexane:EtOAc, 3:1) to get desired product in a light orange color. Yield = 3 g, (42.4%). $^1$H-NMR (DMSO-$d_6$, 300 MHz, $\delta$ in ppm): 9.74 (1H, s, Ar—OH), 7.79 (1H, d, —NHC**CH**), 7.60–7.57 (1H, d, —OHC**CH**), 6.87–6.74 (1H, m, —CH**CH**CH-), 1.46 (9H, s, $-CH_3$).

### 2.4. Synthesis of (E)-tert-butyl(2-hydroxy-5-((4-nitrophenyl)diazenyl) phenyl)carbamate (S2)

4-Nitroaniline (0.5 g, 3.62 mmol) was added to a solution of MeOH:$H_2O$ (1:1). Concentrated HCl (2.0 mL) was added slowly, and the solution was stirred at 0 °C. In order to generate the diazonium salt, an aqueous solution (2 mL) of $NaNO_2$ (300 mg, 4.34 mmol) was added dropwise and stirred for another 15 min at 0 °C. In another RB flask, BOC-protected aminophenol (840 mg, 4.34 mmol) and sodium bicarbonate (1.15 g, 10.8 mmol) were dissolved in MeOH:$H_2O$ (1:1, v/v, 500 mL) and stirred in an ice bath. After 30 min, the diazonium salt solution was added dropwise to the basic solution of aminophenol at 0 °C. The reaction was allowed to stir for 3 h before being poured into water. The pH of the resultant solution was adjusted to neutral to allow for precipitation. A brown-colored solid product was observed, which was collected via filtration. Yield = 1.12 g (90.4%). $^1$H-NMR (DMSO-$d_6$, 300 MHz, $\delta$ in ppm): 11.14 (1H, s, Ar—OH), 8.42–8.39 (3H, d, Ar—H), 8.04–8.01 (2H, d, Ar—H), 7.68–7.64 (1H, d, Ar—H), 7.04–7.01 (1H, d, Ar—H), 1.49 (9H, s, $-CH_3$).

### 2.5. Synthesis of (E)-2-amino-4-((4-nitrophenyl)diazenyl)phenol (Azo)

In a 25 mL round bottomed flask, (E)-*tert*-butyl(2-hydroxy-5-((4-nitrophenyl)diazenyl)phenyl)carbamate (0.1 g, 2.92 mmol) was loaded in 1 mL of anhydrous DCM (dichloromethane). TFA (225 μL) was added dropwise to the solution at 0 °C; after which, the reaction was stirred at room temperature for 4 h. Upon completion, the solvent was evaporated and the residue was extracted using ethyl acetate. The collected organic layer was evaporated under vacuum. Yield = 0.069 g (92%). $^1$H-NMR (DMSO-$d_6$, 300 MHz, $\delta$ in ppm): 11.5 (1H, s, Ar—OH), 8.34 (2H, d, Ar—H), 7.93 (2H, d, Ar—H), 7.25 (2H, d, Ar—H), 6.87 (1H, d, Ar—H), 5.06 (2H, br, Ar—$NH_2$).

### 2.6. Poly(dimethylacrylamide-co-benzophenoneacrylamide-co-vinylbenzaldehyde) [p(DMA-co-VBA)] (P1)

To synthesize this random copolymer via controlled radical polymerization, DMA (3 g, 30.26 mmol), VBA (166 mg, 1.26 mmol), AIBN (2.58 mg, 0.03 mmol), DMP (0.11 g, 0.32 mmol), and DMF (8 mL) were added to Schlenk flask and purged for 30 min under argon atmosphere to remove any dissolved oxygen. Then, the reaction mixture was heated at 60 °C for 12 h. After solvent evaporation, precipitation was encouraged using diethyl ether. $^1$H-NMR (DMSO-$d_6$, 300 MHz, $\delta$ in ppm): 10.01 (1H, s, —CHO), 7.75–7.56 (13H, m, Ar—H), 3.1–2.6 (21H, s, aliphatic H). GPC: $M_n$ = 6650, $M_w$ = 7200, and PDI = 1.1.

### 2.7. Synthesis of P2 via post-modification of P1

P1 and (E) -2-amino-4-((4-nitrophenyl)diazenyl)phenol were taken into ethanol, and $Et_3N$ was added. The reaction mixture was heated at 80 °C for 48 h. After solvent evaporation, precipitation was encouraged using diethyl ether. The precipitate was dried in vacuum to afford P2. $^1$H-NMR (DMSO-$d_6$, 300 MHz, $\delta$ in ppm): 8.34 (2H, d, Ar—H), 7.94–7.52 (15H, br, Ar—H), 7.22 (2H, d, Ar—H), 6.86 (1H, d, Ar—H), 3.2–2.0 (21H, s, aliphatic H). GPC: $M_n$ = 7000, $M_w$ = 7300, and PDI = 1.0.

### 2.8. Sensing studies

A 170 mM stock solution of P2 was prepared in water. Solution samples (10 mM) of the metal ions $Fe^{3+}$, $Li^+$, $K^+$, $Na^+$, $Co^{2+}$, $Cu^{2+}$, $Cd^{2+}$, $Fe^{2+}$, $Al^{3+}$, $Hg^{2+}$, $Zn^{2+}$, $Ni^{2+}$, $Mg^{2+}$, and $Pb^{2+}$ were prepared by dissolving the corresponding salts in water. For the anion studies, stock solutions of the corresponding tetrabutylammonium salts (100 mM) of the anions $F^-$, $Cl^-$, $Br^-$, $I^-$, $CN^-$, $ClO_4^-$, $HSO_4^-$, $CN^-$, $S^{2-}$, $SH^-$, $PO_4^{3-}$, and $SCN^-$ in water were prepared. A 10 μL aliquot of each metal ion and a 5 μL aliquot of each anion's stock solution were added using a microsyringe to a 0.35 mL sample solution of P2 placed in a cuvette. The absorption spectral changes were monitored.

## 3. Results and discussion

Azo-1 (Figure S2) was synthesized via a diazotization reaction

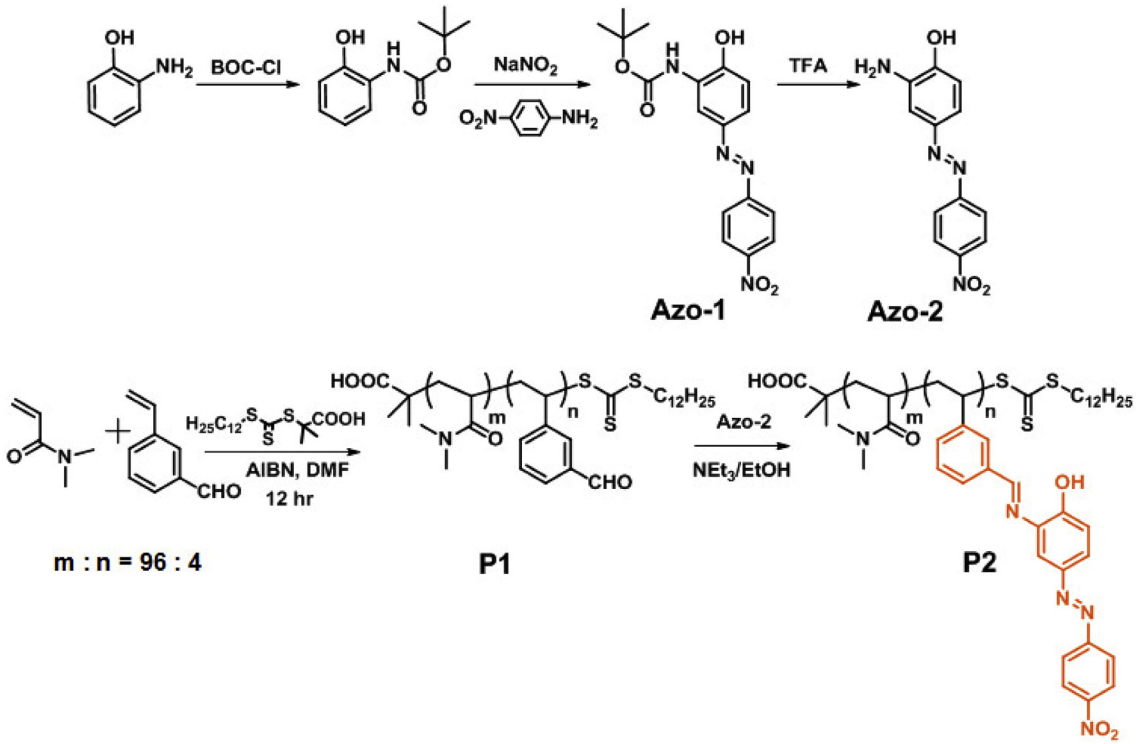


**Scheme 1.** Synthesis of water-soluble polymeric probe (P2) with azo-Schiff base moieties.

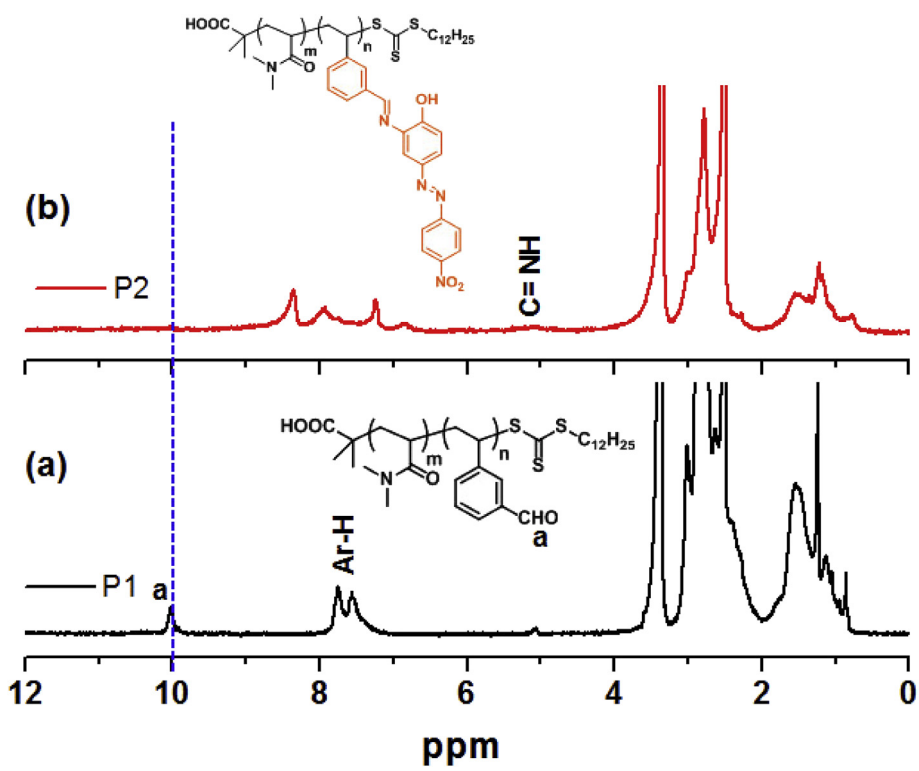


**Fig. 1.** $^{1}$H NMR spectra of (a) P1 and (b) P2.

between BOC-protected 2-aminophenol (Figure S1) and diazonium salt of 4-nitroaniline at 0 °C. Deprotection of the BOC groups in the presence of TFA led to Azo-2. The formation of Azo-2 was monitored using $^{1}$H-NMR spectroscopy (Figure S3). The appearance of aromatic protons in the region of 8.39 to 6.61 ppm and the disappearance of the $-CH_3$ protons on the BOC groups at 1.5 ppm confirmed the successful synthesis of Azo-2.

The design strategy for the synthesis of the azo-Schiff base-derived polymeric probe, P2, is depicted in Scheme 1. A random copolymer, p (DMA-*co*-VBA) (P1), with aldehyde functionalities in the side chains was prepared as reported previously (Fig. 1a) [16]. The incorporation ratio of DMA and VBA along the P1 backbone was 96:4. P1 had a

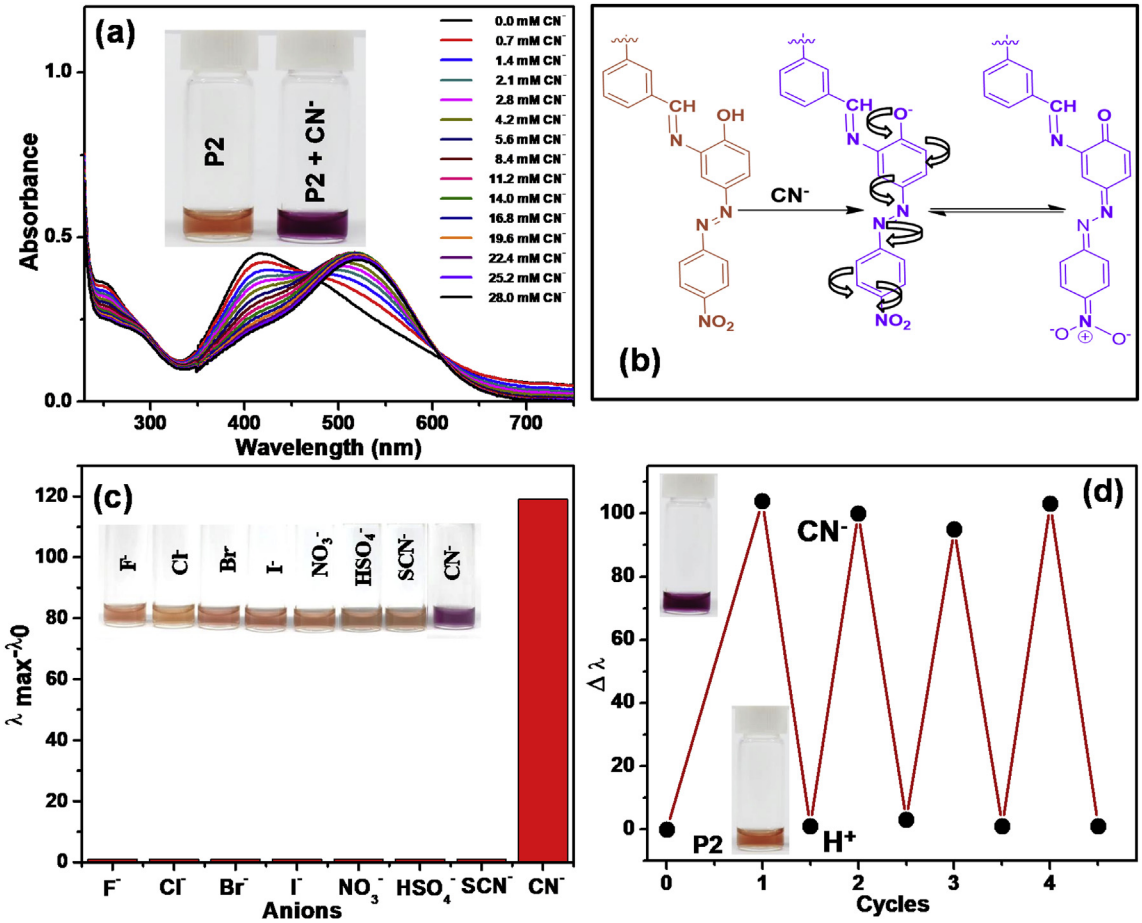


**Fig. 2.** (a) UV–Vis absorption spectra of P2 ($1.52 \times 10^{-5}$ M) upon the gradual addition of $CN^-$ ions at pH 7, (b) plausible mechanism of P2 for the detection of the $CN^-$ ions, (c) selectivity bar diagram of P2 with various anions of tetrabutylammonium (TBA) salts, and (d) reversibility of P2 ($1.52 \times 10^{-5}$ M) upon the alternating addition of $CN^-$ ions and 0.75 (N) HCl in $H_2O$.

$M_n$ = 6650 g/mol and a polydispersity of $M_w/M_n$ = 1.1 (Figure S4). P1 was subjected to a single-step, post-polymerization modification reaction with Azo-2 to obtain P2. The aldehyde group (−CHO) of P1 reacted with amine group of Azo-2 to form P2. The aldehyde peak of P1 at 10.01 ppm disappeared, and the imine proton (−CH=N) of P2 appeared at 5.08 ppm, thus demonstrating complete transformation (Fig. 1b).

The detection of $CN^-$ ions by P2 ($1.52 \times 10^{-5}$ M of azo-chromophore units, assuming 4% incorporation along the backbone) was tested using UV–Vis absorption spectroscopy in aqueous HEPES buffer solution at pH 7 (Fig. 2a). The addition of increasing concentration of $CN^-$ ions up to 28.0 mM caused P2's characteristic absorption maximum to red-shift from 411 to 530 nm. This drastic shift could be observed with the naked eye as a color change from brick-red to purple. This phenomenon could be explained through the abstraction of phenolic protons by $CN^-$ ions, thus leading to the formation of a quinoid structure in presence of electron-withdrawing nitro groups [Fig. 2b] [31]. The lower detection limit for $CN^-$ ions was determined to be 0.1 mM (Figure S5). In order to evaluate the selectivity of P2 towards $CN^-$ ions over the other anions present, the spectral responses of P2 were monitored by screening the other anions, such as $Cl^-$, $F^-$, $Br^-$, $I^-$, $CN^-$, $NO_2^-$, $HSO_4^-$, $S^{2-}$, $SH^-$, $PO_4^{3-}$, and $SCN^-$, using aqueous solutions of their tetrabutylammonium salts (up to 28 mM). The diagram below clearly indicated that P2 selectively detected $CN^-$ ions over all other anions, especially those that did not show any spectral changes (Fig. 2c, Figs. S6-S8). Even though $F^-$ ions were thought to be direct competitors of $CN^-$, our results demonstrated that P2 showed excellent selectivity towards $CN^-$ ions without any interference with $F^-$.

Having examined the colorimetric detection of $CN^-$ ions, pH-dependent sensing studies were conducted (Figs. S9 and S10). P2 showed high sensitivity towards $CN^-$ ions at low to neutral pH where the neutral azo form was dominant. Negligible response was observed at high pH (pH 10 to 12) where the hydrazone form was already generated by deprotonation of the phenolic protons, thereby preventing the detection of $CN^-$ ions. This pH-dependent detection behavior was employed to provide reversibility in the sensing system (Fig. 2d and Fig. S11). The reversible detection process was achieved by decreasing the pH of the solution after the detection of $CN^-$ ions occurred. Once $CN^-$ ions were detected, the absorption band at 530 nm reverted to its original position (411 nm) upon the addition of 0.75 N HCl into the solution. This cycle was repeated four times.

The detection of $Fe^{3+}$ ions by P2 ($1.52 \times 10^{-5}$ M) was also examined using UV–Vis absorption spectroscopy in aqueous HEPES buffer solution at pH 7. Upon the gradual addition of $Fe^{3+}$ ions, a new band appeared at 304 nm with a distinct color change from brick-red to yellow (Fig. 3a). The reason for the large blue-shift of 107 nm in the absorption spectra is due to the formation of a $Fe^{3+}$ ion coordination complex with the lone pair of the O-atom of the hydroxyl group in azo moiety and the N-atom of the imine bond of P2. This inhibited the intramolecular charge transfer process by affecting the electronic environment of the azo-chromophore (Fig. 3b) [33–35]. The detection limit of P2 with $Fe^{3+}$ ions was found to be 0.1 mM (Fig. 3c). The selectivity of P2 was also examined by screening various alkalis, alkalines, and transition metal cations under the same physiological conditions employed for $Fe^{3+}$ ion detection. Fig. 3d represented the selectivity bar diagram of P2 revealed that P2 was highly selective towards $Fe^{3+}$ ions

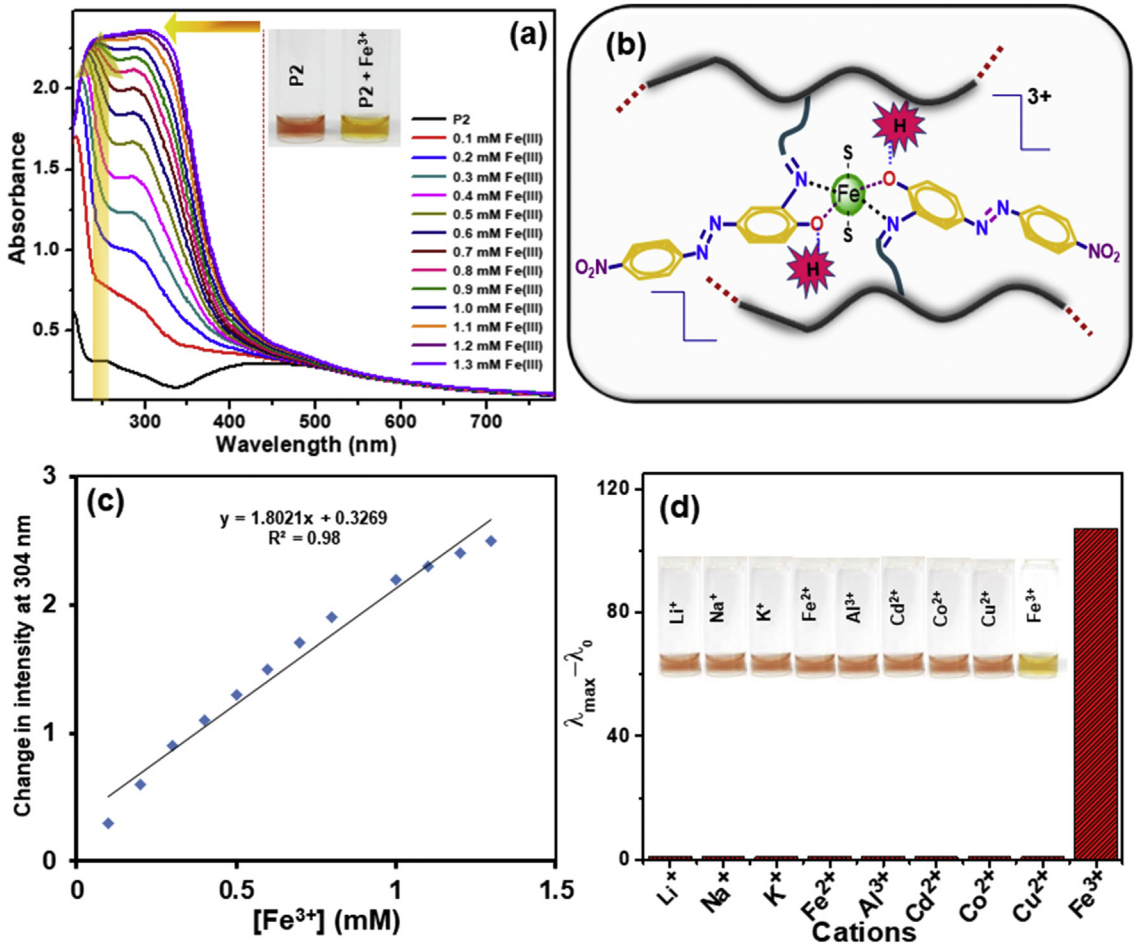


**Fig. 3.** (a) UV–Vis absorption spectra of P2 ($1.52 \times 10^{-5}$ M) upon the addition of $Fe^{3+}$ ions (up to 0.8 mM) in $H_2O$ at pH 7, (b) schematic representation for the formation of the coordination complex of $Fe^{3+}$ ions with P2, (c) a linear regression curve for the calculation of lower detection limit for $Fe^{3+}$ ions, and (d) selectivity bar diagram for different cations (up to 0.8 mM).

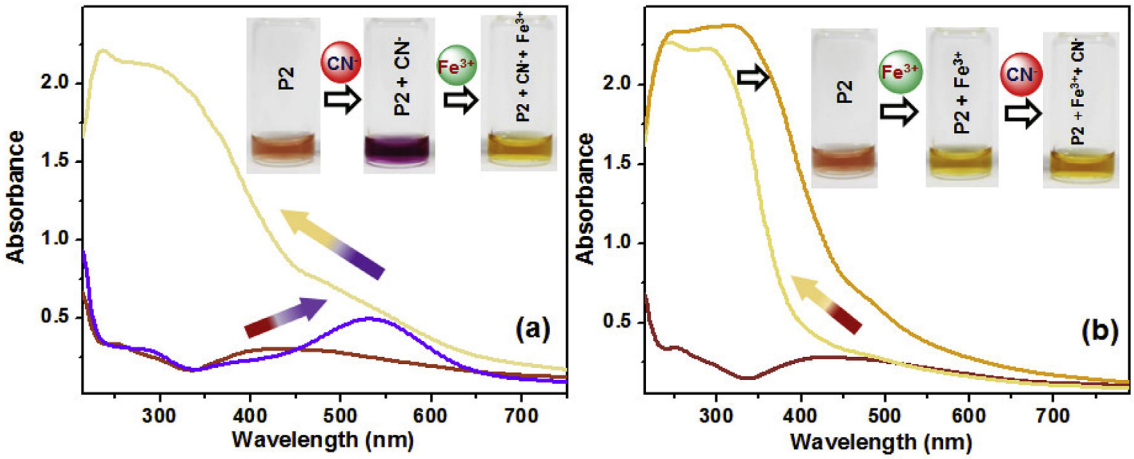


**Fig. 4.** UV–Vis absorption spectra of P2 ($1.52 \times 10^{-5}$ M) upon the addition of (a) $CN^-$ ions followed by $Fe^{3+}$ ions, and (b) $Fe^{3+}$ ions followed by $CN^-$ ions in water.

over other metal cations. The UV–Vis absorption spectral responses of P2 towards metal cations $Li^+$, $K^+$, $Na^+$, $Co^{2+}$, $Cu^{2+}$, $Cd^{2+}$, $Fe^{2+}$, $Al^{3+}$, $Hg^{2+}$, $Zn^{2+}$, $Ni^{2+}$, $Mg^{2+}$, and $Pb^{2+}$ were shown in Figures S12 - S14. Metal binding studies of P2 for $Fe^{3+}$ ions were performed under different pH conditions (Figure S15). No significant change was found in absorption spectra of P2 upon the addition of $Fe^{3+}$ ions at various pH values.

After investigating the proclivity of P2 towards $CN^-$ and $Fe^{3+}$ ions individually, consecutive sensing studies were performed by monitoring the changes in absorbance spectra with the sequential addition of each ion. The addition of $CN^-$ ions to P2 solution has exhibited a red-shift from 411 to 530 nm along with an intense color change from brick-red to purple. The sequential addition of $Fe^{3+}$ ions into the solution of P2 + $CN^-$ ions prepared *in situ* showed a blue-shift from 530 to 304 nm with a color change from purple to yellow (Fig. 4a). In the alternative sequence, the blue-shift appeared with a color change from brick-red to

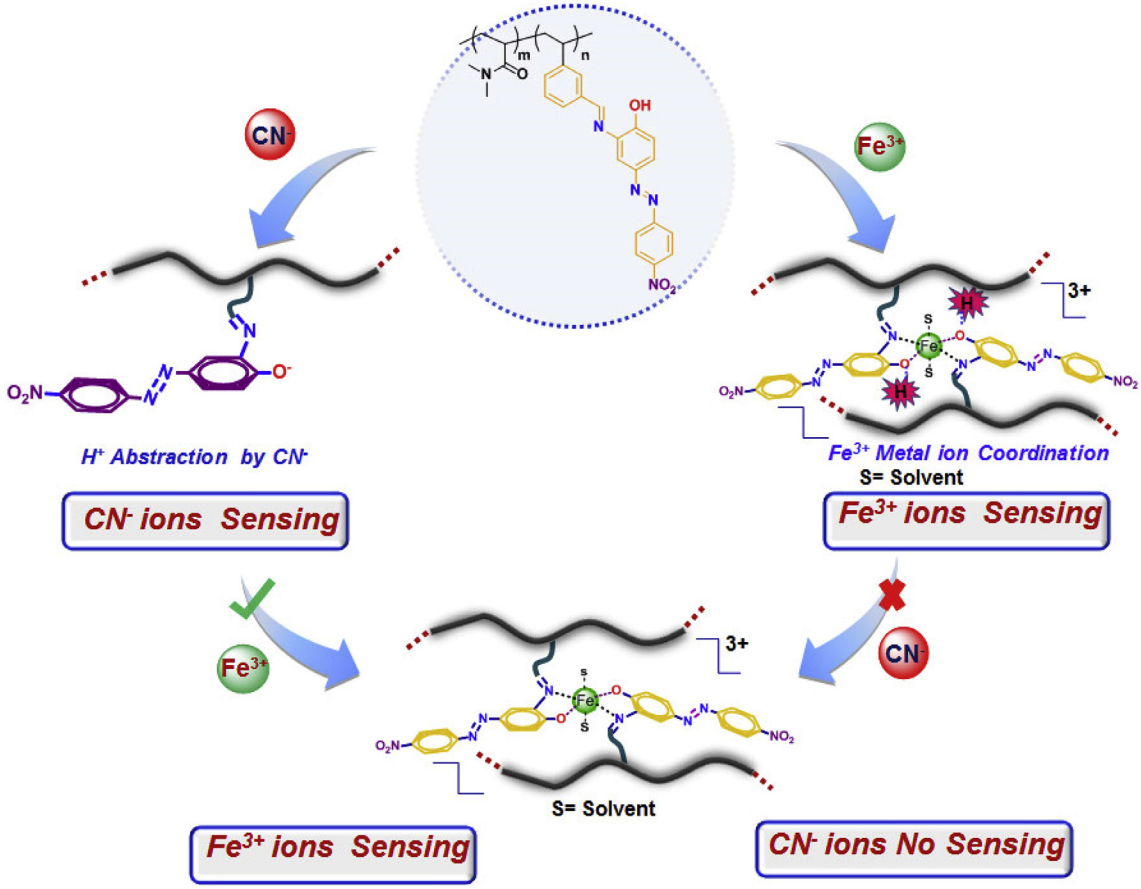


**Fig. 5.** Schematic representation for the plausible mechanism of the consecutive sensing study of P2 with $CN^-$ and $Fe^{3+}$ ions in water.

yellow upon the addition of $Fe^{3+}$ ions. However, no further shifts were found in the absorbance spectra of the aqueous solution of P2 + $Fe^{3+}$ prepared *in situ* after the addition of $CN^-$ ions (Fig. 4b). These results revealed that P2 acted as a dual sensor with distinct color changes only when $CN^-$ ions were added followed by $Fe^{3+}$ ions. The plausible mechanism behind these phenomena is depicted in Fig. 5. After the detection of $CN^-$ ions, the quinoid chromophore formed *in situ* was expected to coordinate with $Fe^{3+}$ ions through the lone pair of O-atom and N-atom of the imine bond. Thus, the addition of $Fe^{3+}$ ions to the P2 + $CN^-$ solution resulted in further color changes from purple to yellow, which in turn enabled the consecutive detection of $CN^-$ and $Fe^{3+}$ ions. However, after the detection of $Fe^{3+}$ ions via the coordination complex, addition of $CN^-$ ions to the P2—$Fe^{3+}$ complex formed *in situ* did not lead to a distinct color change. Though regardless of the ability of the $CN^-$ ions to abstract the phenolic proton of the P2-$Fe^{3+}$ complex, the intense color of the P2-$Fe^{3+}$ complex present in the medium suppressed any color changes caused by elongated conjugation.

## 4. Conclusions

A polymeric probe, P2, based on the Schiff-base unit with azo moiety was developed for the colorimetric detection of $Fe^{3+}$ ions and $CN^-$ ions in aqueous media. P2 showed dual sensing for $Fe^{3+}$ ions and $CN^-$ ions in water with high selectivity and sensitivity. For the $CN^-$ ions sensing studies, P2 showed a red-shift of 119 nm with a distinct color change from brick-red to purple. $CN^-$ ions could be reversibly detected by decreasing the pH of the solution after the detection of $CN^-$ ions. The colorimetric sensing of the $Fe^{3+}$ ions was accomplished by a 107 nm blue-shift in the absorption band with a visible color change from brick-red to yellow due to the formation of coordination complexes between $Fe^{3+}$ ions and azo Schiff-base ligands of P2. Lastly, the sequential sensing studies revealed that the detection of $CN^-$ ions followed by $Fe^{3+}$ ions was possible via the change in color from brick-red to purple to yellow. Addition of the ions in the reverse sequence was unsuccessful because the yellow-colored solution after the formation of P2—$Fe^{3+}$ complex suppressed any color changes caused by the quinoid structure after the addition of $CN^-$ ions.

## Acknowledgements

This work was supported by the Basic Science Research Program (NRF-2017R1A2B4003861) administered by the National Research Foundation of Korea, funded by the Ministry of Science, ICT, and Future Planning of Korea.

## Appendix A. Supplementary data

Supplementary data to this article can be found online at https://doi.org/10.1016/j.dyepig.2019.04.010.

## References

[1] Carter KP, Young AM, Palmer AE. Fluorescent sensors for measuring metal ions in living systems. Chem Rev 2014;114:4564–601.
[2] Kim HN, Lee MH, Kim HJ, Kim JS, Yoon J. A new trend in rhodamine-based chemosensors: application of spirolactam ring-opening to sensing ions. Chem Soc Rev 2008;37:1465–72.
[3] He L, Liu C, Xin JH. A novel turn-on colorimetric and fluorescent sensor for $Fe^{3+}$ and $Al^{3+}$ with solvent-dependent binding properties and its sequential response to carbonate. Sensor Actuator B Chem 2015;213:181–7.
[4] Xu Z, Chen X, Kim HN, Yoon J. Sensors for the optical detection of cyanide ion. Chem Soc Rev 2010;39:127–37.
[5] Yang Y, Zhao Q, Feng W, Li F. Luminescent chemodosimeters for bioimaging. Chem Rev 2013;113:192–270.

[6] Mao J, Wang L, Dou W, Tang X, Yan Y, Liu W. Tuning the selectivity of two chemosensors to Fe(III) and Cr(III). Org Lett 2007;9:4567–70.
[7] Burdo JR, Connor JR. Brain iron uptake and homeostatic mechanisms: an overview. Biometals 2003;16:63–75.
[8] Bonda DJ, Lee H-g, Blair JA, Zhu X, Perry G, Smith MA. Role of metal dyshomeostasis in Alzheimer's disease. Metall 2011;3:267–70.
[9] Gao G-y, Qu W-j, Shi B-b, Lin Q, Yao H, zhang Y-m, et al. A reversible fluorescent chemosensor for iron ions based on 1H-imidazo [4,5-b] phenazine derivative. Sensor Actuator B Chem 2015;213:501–7.
[10] Razi SS, Ali R, Srivastava P, Misra A. Simple Michael acceptor type coumarin derivedturn-onfluorescence probes to detect cyanide in pure water. Tetrahedron Lett 2014;55:2936–41.
[11] Gupta VK, Singh AK, Gupta N. Colorimetric sensor for cyanide and acetate ion using novel biologically active hydrazones. Sensor Actuator B Chem 2014;204:125–35.
[12] Lee SA, You GR, Choi YW, Jo HY, Kim AR, Noh I, et al. A new multifunctional Schiff base as a fluorescence sensor for Al3+ and a colorimetric sensor for CN− in aqueous media: an application to bioimaging. Dalton Trans 2014;43:6650–9.
[13] Jung HS, Han JH, Kim ZH, Kang C, Kim JS. Coumarin-Cu(II) ensemble-based cyanide sensing chemodosimeter. Org Lett 2011;13:5056–9.
[14] Cho EJ, Ryu BJ, Lee YJ, Nam KC. Visible colorimetric fluoride ion sensors. Org Lett 2005;7:2607–9.
[15] Haldar U, Lee H-i. BODIPY-derived multi-channel polymeric chemosensor with pH-tunable sensitivity: selective colorimetric and fluorimetric detection of $Hg^{2+}$ and $HSO_4^-$ in aqueous media. Polym Chem 2018;9:4882–90.
[16] Gupta M, Lee H-i. A pyrene derived $CO_2$-responsive polymeric probe for the turn-on fluorescent detection of nerve agent mimics with tunable sensitivity. Macromolecules 2017;50:6888–95.
[17] Gupta M, Balamurugan A, Lee H-i. Azoaniline-based rapid and selective dual sensor for copper and fluoride ions with two distinct output modes of detection. Sensor Actuator B Chem 2015;211:531–6.
[18] Gupta M, Lee PH-i. A dual responsive molecular probe for the efficient and selective detection of nerve agent mimics and copper (II) ions with controllable detection time. Sensor Actuator B Chem 2017;242:977–82.
[19] Na YJ, Park GJ, Jo HY, Lee SA, Kim C. A colorimetric chemosensor based on a Schiff base for highly selective sensing of cyanide in aqueous solution: the influence of solvents. New J Chem 2014;38:5769–76.
[20] Santos-Figueroa LE, Moragues ME, Climent E, Agostini A, Martínez-Máñez R, Sancenón F. Chromogenic and fluorogenic chemosensors and reagents for anions. A comprehensive review of the years 2010–2011. Chem Soc Rev 2013;42:3489–613.
[21] Balamurugan A, Lee H-i. Aldoxime-derived water-soluble polymer for the multiple analyte sensing: consecutive and selective detection of $Hg^{2+}$, $Ag^+$, $ClO^-$, and cysteine in aqueous media. Macromolecules 2015;48:3934–40.
[22] Choudhury Neha, Saha Biswajit, Bhuban Ruidas, De Priyadarshi. Dual-action polymeric probe: turn-on sensing and removal of $Hg^{2+}$; chemosensor for $HSO_4^-$. ACS. Appl. Polym. Mater. 2019;1:461–71.
[23] Trigo-López M, Muñoz A, Ibeas S, Serna F, García FC, García JM. Colorimetric detection and determination of Fe(III), Co(II), Cu(II) and Sn(II) in aqueous media by acrylic polymers with pendant terpyridine motifs. Sensor Actuator B Chem 2016;226:118–26.
[24] Kamacı M, Kaya İ. A highly selective, sensitive and stable fluorescent chemosensor based on Schiff base and poly(azomethine-urethane) for $Fe^{3+}$ ions. J Ind Eng Chem 2017;46:234–43.
[25] Vallejos S, Muñoz A, García FC, Colleoni R, Biesuz R, Alberti G, et al. Colorimetric detection, quantification and extraction of Fe(III) in water by acrylic polymers with pendant Kojic acid motifs. Sensor Actuator B Chem 2016;233:120–6.
[26] Qin C, Cheng Y, Wang L, Jing X, Wang F. Phosphonate-functionalized polyfluorene as a highly water-soluble iron(III) chemosensor. Macromolecules 2008;41:7798–804.
[27] Saha S, Ghosh A, Mahato P, Mishra S, Mishra SK, Suresh E, et al. Specific recognition and sensing of $CN^-$ in sodium cyanide solution. Org Lett 2010;12:3406–9.
[28] Liu H-B, Han H-S, Lan B, Xiao D-M, Liang J, Zhang Z-Y, et al. Cobalt metal-mixed organic complex-based hybrid micromaterials: ratiometric detection of cyanide. RSC Adv 2018;8:4900–4.
[29] Cho D-G, Kim JH, Sessler JL. The Benzil−Cyanide reaction and its application to the development of a selective cyanide anion indicator. J Am Chem Soc 2008;130:12163–7.
[30] Chakraborty C, Bera MK, Samanta P, Malik S. Selective detection of cyanide by a polyfluorene-based organoboron fluorescent chemodosimeter. New J Chem 2013;37:3222–8.
[31] Mohammadi A, Jabbari J. Simple naked-eye colorimetric chemosensors based on Schiff-base for selective sensing of cyanide and fluoride ions. Can J Chem 2016;94:631–6.
[32] Zhang P, Shi B-B, Wei T-B, Zhang Y-M, Lin Q, Yao H, et al. A naphtholic Schiff base for highly selective sensing of cyanide via different channels in aqueous solution. Dyes Pigments 2013;99:857–62.
[33] Ghosh K, Rathi S. A novel probe for selective colorimetric sensing of Fe(II) and Fe(III) and specific fluorometric sensing of Fe(III): DFT calculation and logic gate application. RSC Adv 2014;4:48516–21.
[34] You GR, Park GJ, Lee SA, Ryu KY, Kim C. Chelate-type Schiff base acting as a colorimetric sensor for iron in aqueous solution. Sensor Actuator B Chem 2015;215:188–95.
[35] Choi YW, Park GJ, Na YJ, Jo HY, Lee SA, You GR, et al. A single schiff base molecule for recognizing multiple metal ions: a fluorescence sensor for Zn(II) and Al(III) and colorimetric sensor for Fe(II) and Fe(III). Sensor Actuator B Chem 2014;194:343–52.